



How do soil and topographic drivers determine tree diameter spatial distribution in even aged cork oak stands installed in average to high productivity areas

Paulo Neves Firmino¹ · Joana Amaral Paulo² · António Lourenço³ · Margarida Tomé² · Manuel Campagnolo²

Received: 4 December 2023 / Accepted: 17 April 2024
© The Author(s) 2024, Corrected publication 2024

Abstract

Local terrain or microsite conditions influence the development of trees, particularly at early ages. These conditions might be described by edaphic or topographic variables. We mapped soil and topographic variables from four even-aged and even-spaced cork oak plantations located in two climatically distinct Portuguese regions. The major goal of this research was to understand the relation between soil and topographic fine-scale conditions and tree growth expressed by diameter without cork annual growth (*idu*). The methodology consisted in (1) analysing the spatial variability and autocorrelation of *idu*; (2) modelling *idu* with ordinary least squares (OLS) regressions; (3) comparing with spatial modelling of *idu*, incorporating spatial autocorrelation. The driest stands A and B, exhibited weaker spatial autocorrelation, distributed in smaller clusters ($R^2 < 0.03$, OLS models), while stands C ($R^2 = 0.18$, OLS models) and D ($R^2 = 0.11$, OLS models) showed higher predictive capacity. Spatial models increased R^2 scores, keeping most variables from OLS models and accounting for spatial autocorrelation. A + B + C + D OLS model obtained an $R^2 = 0.34$ and respective spatial model $R^2 = 0.58$. Apparent electrical conductivity at 0.5 (ECa0.5) and 1 m of soil depth, slope, elevation and topography position index were included as predictors (OLS), but only ECa0.5, slope and elevation were selected in the spatial model. Models were fitted using average to high productivity stands and should be used cautiously outside this range. Local terrain conditions determine the growth of young cork oak trees. Mapping soil and topographic variables before establishing new plantations may identify limiting microsite conditions where using cork oak species is not suitable due to low growth rates expectations.

Keywords Forest plantations · Site index · Spatial correlation · Soil apparent electrical conductivity · Topographic index · Soil digital mapping

Introduction

At early ages trees may be affected by stand density, tree genetics, intraspecific and inter-specific competition, as well as soil and climate microsite conditions (Tomé and Burkhart 1989; Bullock and Burkhart 2005). These drivers are crucial not only for the individual tree growth but also for the whole spatiotemporal ecological dynamics that will be created with age progression (Costa et al. 2009; Andivia et al. 2015). Forest management options and planning are critical for aiming at successful sustainable production stands, in which the cork oak (*Quercus suber* L.) plantations for cork production are included. Young cork oak plantations average a stand density of 500 trees ha⁻¹ (AIFF 2010), but mature cork oak stands are typically found in densities lower than 120 trees ha⁻¹ (ICNF 2019). While for the majority of forest species timber is frequently one of the main productions, for cork oak species timber production is not considered since the cutting down trees is prohibited by Portuguese law. Cork oak stands are managed as agrosilvopastoral systems called montado, with the main product obtained being cork, thus the success and profitability of these systems depend on the management options at early stages (Natividade 1950).

Even though the species is adapted to the summer drought, typical in the Mediterranean climate, the severity of the drought impacts not only cork oak development but also its distribution (Costa et al. 2008; Paulo et al. 2015; Vessella et al. 2017). Climate associated with site factors are determinant to obtain equilibrium in the hydromorphic soil conditions, a relation between soil, topography, and water availability that is essential for the successful cork oak development (Costa et al. 2010). Although a few suitability maps based soil and climate have been developed (e.g. Paulo et al. 2015, 2021), currently these aspects are frequently overlooked during the establishment of new cork oak plantations, as Portuguese regulations are defined for a national application and cork oak is considered a species of interest across the whole country (Coelho et al. 2012).

Tree species development is monitored by measuring tree growth at regular time intervals. Growth related measurements are focused on size characteristics such as tree diameter at breast height, total height or crown radius (e.g. Paulo and Tomé 2009; Li et al. 2019; Maleki et al. 2020). Tree diameter measuring is an easy method to obtain a standardized comparison between individuals or populations, identify patterns and trends (Bullock and Burkhart 2005; Li et al. 2019). The individual variation of oak diameter growth may be affected by tree genetics (Sampaio et al. 2021), competition (Paulo et al. 2002; Gea-Izquierdo and Cañellas 2009), management options (Faia et al. 2019; Lecomte et al. 2022), but also by edaphic and topographic conditions (Brown and Fredericksen 2008; Costa et al. 2008).

Topography has a direct effect on infiltration and runoff through their influence on superficial or underground water flow, which will impact soil properties (Rodrigues et al. 2021). Both topographic and soil characteristics impact water availability and water distribution (Walker and del Moral 2003). Surveying the local variation of these factors can become cost and time demanding, particularly when considering soil sampling. Remote sensing techniques come as a relatively inexpensive alternative to fast map continuous areas. Digital mapping of topography is a common practice in forestry assessment (e.g. Davis and Goetz 1990; Plant 2019; Rocha et al. 2020). Electromagnetic-induction-based methods are techniques to reliably characterize soil property variations in a mobile and non-invasive way. These methods sense soil apparent electrical conductivity (ECa), the ability of soil to conduct an electrical current (Corwin and Lesch 2005). Applications of ECa measurements largely include precision agriculture, aiming at optimizing soil

sampling strategies, delineating soil management zones or predicting yield variability (Kühn et al. 2009; Rudolph et al. 2016; Plant 2019). As for precision forest few applications are found, being mainly related to understanding soil properties (Mcbride et al. 1990; Paillet et al. 2010).

Spatial relations between individual diameter size are found in forest stands (Getzin et al. 2008; Petritan et al. 2012). The distribution patterns and neighbourhood relationships are important aspects of forest spatial structure. While the distribution patterns reflect the spatial distribution of individual plants, neighbourhood relationships describe fine-scale spatial relations of a small group of individuals, including the structural characteristics of several adjacent trees surrounding a reference tree (Li et al. 2019). These spatial patterns result from the adaptation of trees to their surrounding conditions, exhibiting usually position spatial autocorrelation patterns (Reed and Burkhart 1985; Sedda et al. 2011). Fine-scale variations of soil and topography related factors may trigger spatial correlation on trees, along with sunlight or nutrient availability, potentially creating spatial patterns of tree characteristics within the stand.

Some studies have been centred on understanding spatial patterns on cork oak development (e.g., Costa and Oliveira 2001; Costa et al. 2008; Dettori et al. 2018; Sampaio et al. 2021). Few have applied spatial analysis of cork oak individuals on continuous stands, based on tree height (Sedda et al. 2011), crown diameter (Paulo et al. 2002) or diameter (Sedda and Dettori 2006). None have used multiple stands to verify the possibility of responses of cork oak individuals to site conditions on distinct locations. Our study attempts to fill this gap by understanding how microsite conditions and spatial patterns may determine tree diameter on young cork oak plantations. Our work aims thus to 1) examine the relationships between young cork oak diameter and microsite conditions; 2) identify and analyse the presence of spatial correlation in individual tree diameter 3) quantify the benefits of integrating spatial correlation in tree diameter growth modelling.

Materials

Stands description

Four pure even-aged regular cork oak plantations were selected for tree measurement and soil variable collection according to their productivity. These stands contain part of the network of long-term permanent inventory plots from the ForChange research group (Centro de Estudos Florestais; Instituto Superior de Agronomia), established in cork oak juvenile plantations. Stands contained between two and four 2000 m² rectangular inventory plots, attempting to cover most of the variability observed in tree development. According to the permanent plots site index (S) values, the four stands showed average to high productivities (Paulo et al. 2015). Trees were either debarked or were first debarked less than five years ago when the tree measurement occurred, thus were considered as juvenile trees characterized by a linear diameter growth trend (Paulo and Tomé 2009; Firmino et al. 2023). Stand A (5.3 ha) and B (6.5 ha) were situated in Santarém district, while stands C (4.2 ha) and D (3.9 ha) were in Castelo Branco district, Portugal (Fig. 1). Soil information was already available from previous characterization of the permanent plots by examination of opened soil profiles (Paulo et al. 2015), providing a description of usable soil depth and root system depth. This information was complemented with the FAO soil group from the IUSS Working Group WRB (2006) classification. Four soil profiles had been opened in stand B and

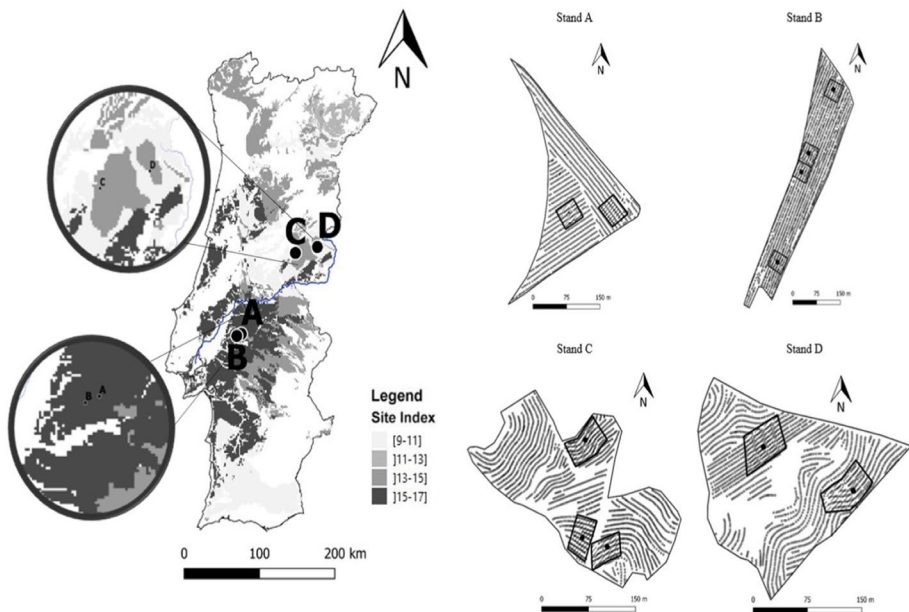


Fig. 1 Characterization of the four sampled stands, A, B, C and D: Left, localization along with the estimated site index map produced by Paulo et al. (2015); Right, spatial arrangement of each stand, along with the location of the existing permanent inventory plots and soil profiles. Individual tree and soil profile locations are represented by (●) and (•), respectively

C, two in stand D. Stand A, having no soil profile opened, was classified according to the FAO soil group. Stand and climatic characterization is shown in Table 1, displaying stand age, density, site index, climatic variables and usable soil depth and soil classification. Site

Table 1 Site and cork oak stand characterization from stand A, B, C and D, according to the existing long-term permanent inventory plots

| | A | B | C | D |
|-------------------------|------------------|---------------------|-----------|-----------|
| t | 20 | 28 | 28 | 16 |
| N | 233 | 235 | 353 | 445 |
| S | 18.4 | 17.0 | 14.7 | 15.7 |
| Soil FAO classification | Arenosols | Arenosols/Cambisols | Cambisols | Cambisols |
| Usable soil depth | 1.00 (estimated) | 1.05–1.70 | 0.45–1.30 | 0.70–0.85 |
| Mean temperature | 16.8 | 16.8 | 15.9 | 15.9 |
| Annual Precipitation | 643.1 | 643.1 | 768.8 | 768.8 |

Where t is the age of the stand, in years; N is the stand density given by the living trees per hectare; S is the site index value (m), estimated with the model developed by Sánchez-González et al. (2005); Soil FAO classification is the classification according to the IUSS Working Group WRB (2006); Usable soil depth is the depth which the root system is able to develop and mean annual temperature (°C) and annual precipitation (mm), were obtained according to the climatic normals of 1981–2010 provided by the Instituto Português do Mar e da Atmosfera (IPMA)

index was calculated for a base age of 80 years, determined by the height growth model for dominant cork oak trees from Sánchez-González et al. (2005). Annual precipitation and average temperature are from the 1981–2010 climate normals, provided by the Instituto Português do Mar e da Atmosfera (IPMA), available at [www.http://portaldoclima.pt/](http://portaldoclima.pt/).

Tree measurements

Every tree was georeferenced, and the respective diameter was measured at breast height above cork. Absent trees in the plantation were considered mortality and excluded from the analysis. Plants without measurable diameter at 1.30 m were found in stand B (1.8%), stand C (10.9%) and stand D (16.7%), not being considered in our analysis. Diameter without cork (*du*) was either calculated by measuring cork thickness in debarked trees and subtracting it twice to diameter, either estimated by using *du* equation in virgin cork oaks according Paulo and Tomé (2014). Based on the linear growth stage of the tree development that characterizes the juvenile stage of cork oak growth (Faías et al. 2020; Firmino et al. 2023), diameter without cork annual growth (*idu*) was calculated by dividing *du* by the known stand age. Boxplots of *idu* measured in each stand are shown on Fig. 2.

Individual tree crown width, in meters, was estimated based on the diameter measurements, according to the fixed effects models from Paulo et al. (2016). A circular area of influence was calculated for each tree, based on the expected size from the cork oak root

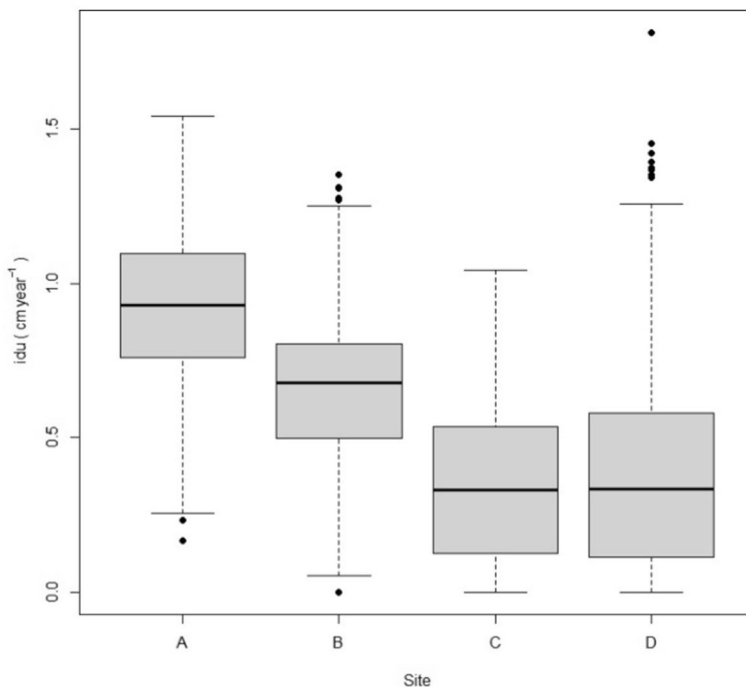


Fig. 2 Boxplot of diameter without cork annual growth (*idu*) for stands A, B, C and D

system. Each area was calculated with a radius equal to 2.5 the average canopy radius of each tree (Moreno et al. 2005; Dinis 2014), previously estimated from tree diameter.

Soil variables

Stand soil characterization was acquired by combining available information from soil pits (Paulo et al. 2015) and data collected in the field. A sensor model EM38-MK2 (Geonics Limited™) was used to obtain apparent electrical conductivity of soil (ECa), defined as the ability of the soil to conduct electric current (Domsch and Giebel 2004; Heil and Schmidhalter 2017). ECa data was collected in the whole stands, allowing the production of detailed soil digital mapping of the stands (Doerge et al. 1999; Machado et al. 2015; Neely et al. 2016). Data was collected less than 48 h after raining, when soil was not excessively moist or dry. One measurement was executed per stand, since soil ECa pattern does not change significantly over time, unless any significant artificial or natural soil movement occurs (Doerge et al. 1999). Elevation mapping was executed simultaneously with a ROVER™ iSurvey SL500 RTK GPS, allowing to create a digital terrain model of each stand. Generated maps, digital terrain models and ECa digital map, had a one-meter pixel size resolution.

Soil variables consisted in the soil apparent electrical conductivity (mS/m) at soil depth of 0.5 m (ECa0.5) and one meter (ECa1). These specific soil depths are known to contain most of cork oak root biomass distribution when considering the soil first depth m (Besson et al. 2014; Dinis 2014), thus soil physical properties at these depths should be of particular interest for tree water absorption.

Topographic variables

The digital terrain model was used to obtain terrain elevation and calculate variables Slope and Aspect. Since elevation impact can be scale-dependent (Príncipe et al. 2022), two distinct variables were considered: the intra-stand variation of elevation (RelElev), standardised as the difference to each stand mean value, as the overall elevation according to the sea level (Elev). The distinction was made so RelElev focused on the fine-scale variation, while Elev, as computed at a broader regional scale. Since aspect in degrees is considered a circular variable, cosine (northerliness) variation was used instead for modelling. Northerliness values range from close to 1, north direction, and -1 if the aspect is southward.

Topographic position index (TPI) was obtained by the difference between the elevation at one position and the mean elevation of its surrounding (Wilson et al. 2007). Positive values indicate higher locations in comparison to its surroundings, negative indicate lower locations and TPI values close to zero represent tendentially flat positions. Topographic Ruggedness index (TRI) is similar to TPI, with the distinction of being expressed as the amount of elevation difference between the surrounding cells instead of the mean (Riley et al. 1999). We attempted to capture fine-scale topographic variations as micro-depressions and small ridges, using the 5×5 surrounding one-meter pixels (Salinas-Melgoza et al. 2018), as our analysis focused on the individual tree and the expected root extent area.

Topographic wetness index (TWI) is defined as the logarithm of the ratio between the local upslope area draining through a certain point per unit contour length and the tangent of the local slope (Beven and Kirkby 1979). It has been widely used to study spatial scale effects on hydrological processes and identify hydrological flow paths, being useful for the characterization of biological processes. Higher TWI values estimate potentially

higher water accumulation at a given location. Terrain variables were calculated with the R software (R Core Team 2021) version 3.6, using raster package, with exception for TWI, calculated using whitebox package (Lindsay 2016).

Every tree position, including living, dead or absent trees, was associated with soil and terrain variables, by attributing the respective location pixel value. Trees within a five-meter proximity from the stand limits were considered as border trees and removed from modelling, minimizing the impact of any external factors that could influence tree development (Sedda et al. 2011).

Methods

Spatial weights matrix

Analysing the spatial patterns in *idu* requires the definition of the spatial weights matrix. This is a $N \times N$ symmetric matrix, with N being the number of individuals, where W_{ij} represents the proximity between individuals (i, j) , which is set to 0 when two individuals are too far apart to be considered spatially related. Notice that individuals which are closer together have higher proximity.

The notion of proximity is usually determined either by the inverse of the distance or spatial lag. The distance can be simply the Euclidean distance between the location of individuals (i, j) up to a user-defined threshold, above which the proximity is set to 0. The spatial lag is computed through a two-step process: firstly a contiguity matrix is defined, where each pair of individuals is either classified as neighbours (1) or not neighbours (0) according to a user-defined rule; then, the spatial lag is the minimum number of spatial units to reach i from j for each pair (i, j) . The weights between each pair of observations indicate the strength of their spatial relationship. Selecting an adequate spatial weights matrix depends on the data itself, on the expected spatial correlations to be captured and on the research question (Fortin and Dale 2005).

This study was based on point data, distributed along lines but not precisely arranged as regular grids, with a varying rate of absent points due to tree mortality and small tree size. As both distance-based measures and contiguity-based measures seemed reasonable to construct the weight matrix, we tested the best distance-based measures up to 15 m, two contiguity-based measures (4 and 8 nearest neighbours) and a more complex approach, based on the potential interaction distance between individuals. The latter approach consisted in defining the potential area of influence of each tree, estimated in section “[Tree measurements](#)” based on the extent of their root system. A pair of trees would be defined as neighbours if their respective areas of influence overlapped (Fig. 3). This approach is based on the principle that contiguity is related to individual tree size, and not just to distance, which has been shown to be a more adequate concept to characterize the interactions between close trees (e.g. Firmino et al. 2023). A row-normalized weights matrix was constructed, where all non-zero weights in each row are equal and their sum is 1. The most suitable spatial weights matrix was selected by analysing its adequacy for capturing the spatial relationships, based on Moran’s I tests statistics and based on the number of neighbours per tree, so that only clearly isolated trees had no neighbours, and the spatial homogeneity of the number of neighbours per tree across the stand area (see Online Resource 1).

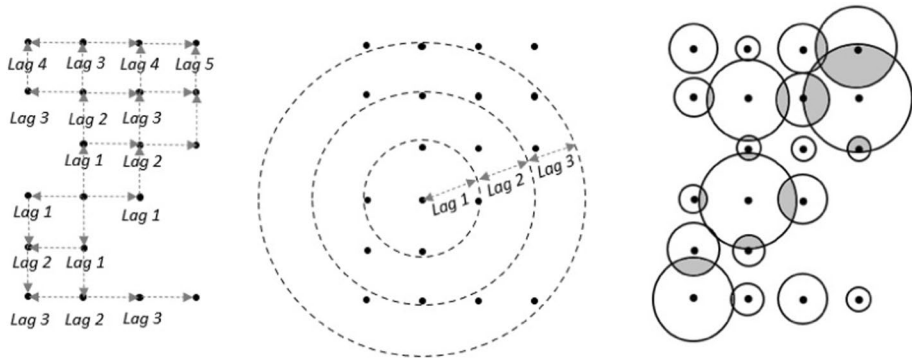


Fig. 3 Scheme of tree neighbour definition according to three approaches for the notion of proximity: Left, contiguity-based approach; Middle, distance-based approach; Right, Area of influence approach, with trees being considered neighbours if the respective areas of influence are overlapped. Lag corresponds to the minimum number of spatial units between a pair of observations, according to the notion of proximity used. Tree locations are represented with (●), tree area of influence with (○) and overlapped areas of influence with (⊙)

Spatial autocorrelation analysis

Spatial autocorrelation was assessed by computing spatial correlograms and using the spatial weights matrix to calculate the Moran's I statistics and fit spatial models.

The Moran's I statistic is an indicator of the global presence of spatial autocorrelation among neighbours. It evaluates whether there is a pattern of similarity or dissimilarity among neighbouring observations, by allowing to test the null hypothesis of absence of spatial autocorrelation (Moran 1950; Bivand and Wong 2018). Moran's I statistic value ranges from -1 , corresponding to the presence of negative autocorrelation, to 1 , positive autocorrelation. A value of zero indicates the absence of spatial correlation. Moran's I is calculated as:

$$I = \frac{n}{\sum_i \sum_j w_{ij}} \frac{\sum_i \sum_j w_{ij} z_i z_j}{\sum_i z_i^2}, \text{ with } z_i = Y_i - \bar{Y}; z_j = Y_j - \bar{Y} \quad (1)$$

where I is the Moran's I statistic, i and j are point locations, n is the number of observations, Y_i and Y_j are variable values at location i and j , respectively, \bar{Y} is the mean of the variable of the n observations and w_{ij} is the ij^{th} element of the spatial weights matrix and represents the proximity between locations i and j . In Eq. 1, the first term is just a normalization term that depends on the scale of the weights. The second term measures correlation between neighbours: the larger the deviation from the mean, the larger the magnitude of the cross-product on the numerator. If no spatial correlation is present, the expected value of I is $-1/(n-1)$, which approaches 0 as n becomes larger.

Spatial correlograms show how the similarity of variable values varies between spatial units as function of a distance concept. They are advantageous to compare spatial autocorrelation between multiple stands, as they use Moran's I statistics, which are standardized (Legendre and Fortin 1989). Spatial correlograms require the definition of spatial units, the lag h . The lag may correspond to a contiguity-based number of nearest neighbours or a distance-based band of defined range as illustrated in Fig. 3. The spatial correlogram is

obtained by computing Moran's I statistic for each lag h , i.e. $I(h)$ is the index I when only pairs (i, j) that are approximately distance h apart are considered. In practice, we consider all pairs of observations whose distance falls within a distance interval with a semi-amplitude of 3.5 m that includes h (see Fig. 5 for correlogram examples). This semi-amplitude was uniform for all the stands to provide an accurate comparison, based on the previously defined notions of proximity in section "Spatial weights matrix".

Spatial versus non-spatial modelling

Our modelling phase consisted in fitting ordinary linear squares (OLS) linear models between *idu* and edaphic and topographic variables.

Predictors used were ECa0.5, ECa1, RelElev, Slope, Aspect, TPI, TRI and TWI for individual stand models, defined as local models. These models focused on inspecting the influence of predictors in each stand, with distinct variable ranges.

The same predictors and a ninth variable, Elev, were used to fit to the full data together, A + B + C + D model, defined as general model. The model aimed at showing the relationship between the response variables and predictors considering a wider range of variables.

If spatial autocorrelation was observed in the data, a spatial modelling approach was also applied. Plants without diameter at breast height were removed from the modelling phase, avoiding homoscedasticity assumption being violated (Myers 1990). The best sub models were selected using the LEAPS algorithm (Furnival and Wilson 1974) with a similar method to Cerasoli et al. (2018). Generated models were compared with the determination coefficient (R^2) and the Akaike's information criterion (AIC).

Spatial lags models (SLM), spatial errors models (SEM) and simultaneous autoregressive models (SAR) were considered as spatial models to fit the data (see Table 2). Lagrange multipliers tests (Anselin et al. 1996; Bivand et al. 2021) are used to check if either these models are useful, by considering a null hypothesis of $\rho=0$ or $\lambda=0$. Four outcomes are possible depending on rejection/non-rejection of the parameters null hypothesis: (1) both tests null hypotheses are rejected, thus OLS model was preferable; (2) one of the null hypothesis $\rho=0$ or $\lambda=0$ is rejected, then the corresponding model is selected; (3) neither test rejects the null hypothesis, then one cannot conclude that both effects (lag and error) are present, since each one of them have power against the other alternative, requiring the robust forms of the tests for SLM and SEM to provide a correction by making an asymptotic adjustment (Anselin et al. 1996); (4) both robust forms of the tests rejects the null hypothesis, the higher-order SAR model became a candidate which is tested with the portmanteau Spatial AutoRegressive Moving Average (SARMA) test (Anselin and Bera 1998; Bivand et al. 2021), for the null hypothesis $\rho=0$ and $\lambda=0$ simultaneously. Finally, if two models showed close scores in Lagrange multipliers/SARMA tests, a likelihood ratio test (Pace and LeSage 2003) was executed to verify if the model with simpler model (SLM/SEM) was equally adequate as the more complex (SAR). If both models were equally adequate, the simpler one was selected.

Residuals homoscedasticity and normality verification guarantees that the dispersion of model residuals does not show a bias or pattern across the predicted values, and that residuals are normally distributed, thus validating the models reliability and accuracy for statistical inference and result interpretation. We checked residuals homoscedasticity and normality by plotting studentized residuals against the predicted values and inspecting the quantile–quantile plot, respectively, for both OLS and spatial models (Myers 1990).

Table 2 Major models considered in this study

| Name | Model | Observations |
|--|---|---|
| Ordinary Linear Regression (OLS) | $Y = X\beta + \varepsilon$ | ε i.i.d, $E[\varepsilon] = 0$, $V[\varepsilon] = \sigma^2 I$ |
| Spatial lag model (SLM) | $Y = \rho WY + X\beta + \varepsilon$ | Y depends explicitly on its neighbours via the term ρWY |
| Spatial error model (SEM) | $Y = X\beta + \eta$, with $\eta = \lambda W\eta + \varepsilon$ | The error term η accommodates the autoregression structure |
| Simultaneous auto-regressive model (SAR) | $Y = \rho WY + X\beta + \eta$, with $\eta = \lambda W\eta + \varepsilon$ | Combines both SLM and SEM models |

Where the term ρW represents the spatial autocorrelation on response variable Y based on the weight matrix W , the term $X\beta$ is the standard term for explanatory variables and the term $\lambda W\eta$ represents the spatial correlation from explanatory variables, with the autoregression coefficient λ associated also to the W weights matrix

The presence of multicollinearity was evaluated since it may lead to unreliable parameter estimation. The Variance Inflation Factor (VIF) was calculated for each predictor, where one represents the absence of multicollinearity, and a value exceeding five leads to inspecting the possibility of removing the variable (Myers 1990).

Statistical analysis was made with the R software (R Core Team 2021) version 3.6, using the following packages: ‘car’ (Fox and Weisberg 2019) for model multicollinearity evaluation; ‘spdep’ (Bivand and Wong 2018) for executing Moran I tests and correlograms; ‘leaps’ for helping find the best subsets on linear model selection (Lumley 2009); ‘spatial-reg’ for fitting spatial models (Bivand et al. 2013).

Results

Spatial autocorrelation analysis

Distance-based proximity measures were the most adequate for capturing spatial autocorrelation in stands A and B, but contiguity-based performed better for stands C and D. Proximity measures based on the tree area of influence showed consistently lower scores. Spatial units with smaller distances showed a better ability to capture spatial autocorrelation in each of the stands (A=6 m; B=7 m; C=4 neighbours; D=4 neighbours), with the number of neighbours in stand A and B varying between zero and five (Fig. 4; Table 3). When considering the spatial autocorrelation from all the stands (A + B + C + D), contiguity-based proximity measures considering four neighbours were more adequate to capture spatial autocorrelation.

All juvenile cork oak stands showed presence of positive spatial autocorrelation (Moran’s I statistic: A=0.177; B=0.192; C=0.295; D=0.323; all P -values < 0.001). By analysing each correlogram, the distance until the *idu* spatial autocorrelation became a random process (no autocorrelation) varied from 20 to 150 m (Fig. 5). The combined data from all stands A + B + C + D showed also a positive spatial autocorrelation (Moran’s I statistic: A=0.547; P -value < 0.001).

Spatial versus non-spatial modelling

A total of 3844 tree diameter measurements were taken across all four stands. Summary statistics for each of the variables collected are presented in Table 4.

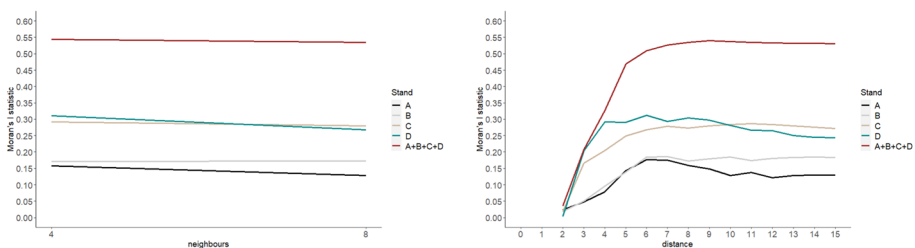


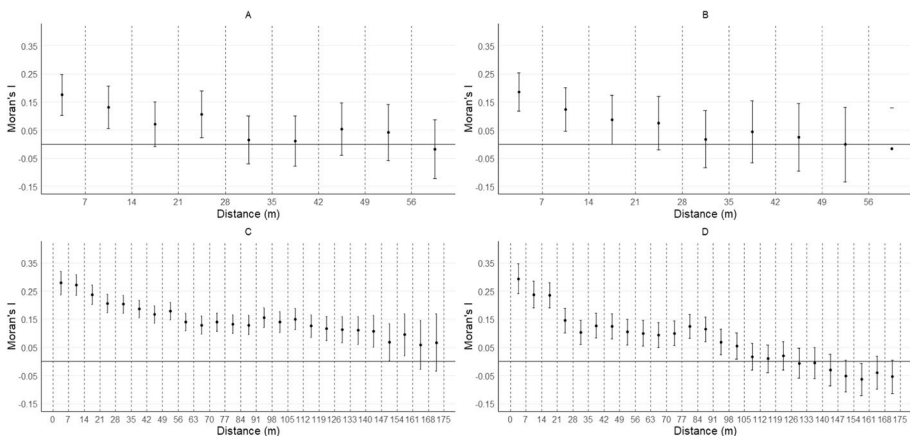
Fig. 4 Moran’s I statistics calculated for each stand (A, B, C and D) and combined data (A + B + C + D) according to: Left, notion of proximity based on contiguity-based measures, for 4, 8 nearest neighbours; Right, notion of proximity based on distance-based measures up to 15 m

Table 3 Moran's I test statistics using spatial weights matrices constructed by six proximity notions: three distance-based measures, 5, 6 and 7 m; two contiguity-based measures, 4 and 8 closest neighbours; the area of influence approach

| Stand | Dist 5 m | Dist 6 m | Dist 7 m | k-neigh 4 | k-neigh 8 | Area of influence |
|---------------|-------------|-------------|-------------|--------------|--------------|-------------------|
| A | 0.143 | 0.176 | 0.175 | 0.158 | 0.128 | 0.087 |
| B | 0.139 | 0.184 | 0.186 | 0.171 | 0.172 | 0.108 |
| C | 0.250 | 0.268 | 0.278 | 0.292 | 0.280 | 0.197 |
| D | 0.291 | 0.312 | 0.294 | 0.310 | 0.268 | 0.273 |
| A + B + C + D | 0.468 | 0.509 | 0.526 | 0.543 | 0.534 | 0.461 |

For each proximity were applied row-normalized weights

No significance information is shown, since all Moran's I tests were significant, with P -value < 0.001

**Fig. 5** Correlograms with Moran's I statistic for diameter without cork (*du*) in the four studied stands. Lags correspond to distance-based bands of 7 m between the lower and upper bounds in which trees are considered neighbours. Horizontal line ($y = 0$) corresponds to the absence of spatial autocorrelation

Terrain variables tested as predictors, when fitted on OLS linear models, showed a very small impact on explaining the cork oak *idu* variability in stands A and B, but some predictive capacity in stand D and particularly in stand C (R^2 : A=0.028; B=0.013; C=0.203; D=0.073). The general model showed a predictive capacity of $R^2 = 0.344$ (Table 5). Fitted OLS models included distinct predictors with each individual stand. The general model, where predictors had a wider range of values, showed ECa0.5 and ECa1 as important variables with estimates of opposite signal, Elevation with a positive parameter estimate, and RelElev, Slope and TPI with negative estimates (Table 5).

Both normality and homoscedasticity assumptions from the residuals were verified on all the fitted models. No multicollinearity was observed between predictors, with VIF values being consistently lower than 5. Autocorrelation was found on individual stand models residuals (Moran I test: A Moran statistic=0.147 $P < 0.001$; B Moran statistic=0.187 $P < 0.001$; C Moran statistic=0.103 $P < 0.001$; D Moran statistic=0.184 $P < 0.001$).

Table 4 Site and cork oak stand traits from stand A, B, C and D: minimum, maximum, mean and standard deviation values

| | | <i>n</i> | <i>du</i> | <i>idu</i> | Elev | Slope | ECa0.5 | ECa1 | TPI | TWI | TRI | Aspect |
|---|------|----------|-----------|------------|------|-------|--------|------|------|------|-----|--------|
| A | Min | 831 | 3.3 | 0.17 | 151 | 0.4 | 2.6 | 3.4 | -2.3 | 3.5 | 0.0 | -1.0 |
| | Max | | 30.8 | 1.54 | 157 | 8.0 | 4.5 | 5.7 | 2.0 | 9.4 | 0.7 | 1.0 |
| | mean | | 18.4 | 0.92 | 155 | 3.9 | 3.3 | 4.1 | -0.1 | 6.1 | 0.3 | 0.0 |
| | Sd | | 4.8 | 0.24 | 1.3 | 1.5 | 0.3 | 0.4 | 1.0 | 0.9 | 0.2 | 0.7 |
| B | Min | 1131 | 0.0 | 0.0 | 132 | 1.9 | 2.5 | 2.8 | -2.2 | 3.6 | 0.0 | -1.0 |
| | Max | | 37.9 | 1.35 | 148 | 19.4 | 5.1 | 6.8 | 2.1 | 8.8 | 2.4 | 1.0 |
| | mean | | 18.0 | 0.64 | 140 | 7.4 | 3.3 | 3.9 | 0.2 | 5.6 | 0.5 | 0.0 |
| | Sd | | 6.9 | 0.25 | 3.7 | 2.3 | 0.4 | 0.6 | 0.9 | 0.9 | 0.3 | 0.7 |
| C | Min | 1041 | 0.0 | 0.00 | 386 | 0.1 | 0.8 | 1.5 | -0.8 | 1.1 | 0.0 | -1.0 |
| | Max | | 29.5 | 1.05 | 397 | 20.6 | 7.1 | 9.2 | 0.5 | 14.1 | 2.3 | 1.0 |
| | mean | | 9.6 | 0.34 | 392 | 4.2 | 2.9 | 3.4 | -0.1 | 5.8 | 0.4 | 0.0 |
| | Sd | | 6.9 | 0.25 | 2.5 | 2.0 | 1.2 | 1.2 | 0.1 | 1.5 | 0.3 | 0.7 |
| D | Min | 841 | 0.0 | 0.00 | 430 | 0.1 | 1.6 | 4.6 | -0.4 | 2.6 | 0.0 | -1.0 |
| | Max | | 22.7 | 1.42 | 441 | 16.7 | 4.9 | 10.0 | 0.6 | 16.7 | 1.7 | 1.0 |
| | mean | | 5.8 | 0.37 | 436 | 3.7 | 3.1 | 6.3 | 0.1 | 6.0 | 0.4 | 0.0 |
| | Sd | | 4.9 | 0.31 | 3.4 | 2.0 | 0.5 | 1.0 | 0.1 | 1.6 | 0.2 | 0.7 |

Where *n* is the number of trees measured per stand, *du* is the individual diameter without cork (cm), *idu* is the individual annual diameter growth without cork (cm year⁻¹), Elev is terrain elevation (m), Slope (%), soil apparent electrical conductivity at 0.5 m (ECa0.5) and 1 m (ECa1) of soil depth (mS/m), Topographic position index (TPI), Topographic ruggedness index (TRI) and Topographic wetness index (TWI) and Aspect (cosine of aspect). TPI, TRI, TWI and Aspect are dimensionless

Spatial modelling incorporated the observed spatial autocorrelation on the fitted OLS models. The simpler model SEM was selected for stand A, but SAR performed better in stands B, C and D. All spatial models included the same respective OLS variables and similar estimates, with exception of TPI variable in stand A. All R^2 scores improved with the spatial models (Table 6). CEa0.5, Elev and Slope were the variables kept in SAR, the best performing spatial model for A + B + C + D. Model assumptions were verified, including the absence of spatial autocorrelation on the residuals (Moran's I test on model residuals: A, $P=0.573$; B, $P=0.594$; C, $P=0.558$; D, $P=0.558$; A + B + C + D, $P=0.879$).

Discussion

Spatial correlation analysis

This study has shown that spatial analysis tools are useful resources to explore underlying within-stand patterns of cork oak *idu*. Spatial weights matrices showed that shorter lags were more appropriate to identify spatial autocorrelation on cork oak growth, independently of being distance-based or contiguity-based. Using an area of influence metric to account for neighbours showed an overall lower ability to detect spatial autocorrelation, possibly due to the range of tree diameters in the stands. Stands with higher average *du* showed a large difference in the detection of spatial autocorrelation compared to

Table 5 Ordinary least squares model and simultaneous autoregressive model (SAR) estimates and statistics for the four individual stands (A, B, C and D) and the combined data (A+B+C+D). DF is the Degrees of Freedom, R^2 is the model coefficient of determination and AIC is the Akaike's information criterion

| Stand | Model | Predictor | Estimates | DF | R^2 | AIC |
|---------------|------------------|-----------|-------------|------|-------|---------|
| A | OLS linear model | Intercept | 0.861*** | 826 | 0.028 | − 16.8 |
| | | Eca0.5 | − 0.157*** | | | |
| | | Eca1 | 0.098** | | | |
| | | TPI | − 0.160* | | | |
| | | TWI | 0.027** | | | |
| | SEM model | Intercept | 0.873*** | 825 | 0.052 | − 30.1 |
| | | Eca0.5 | − 0.151** | | | |
| | | Eca1 | 0.095* | | | |
| B | OLS linear model | TWI | 0.024* | 1128 | 0.010 | − 80.2 |
| | | Intercept | 0.632*** | | | |
| | | Slope | 0.023** | | | |
| | SAR model | TRI | − 0.158** | 1125 | 0.074 | − 113.4 |
| | | Intercept | 0.677*** | | | |
| | | Slope | 0.024** | | | |
| C | OLS linear model | TRI | − 0.163** | 1038 | 0.177 | − 309.4 |
| | | Intercept | − 9.546*** | | | |
| | | Eca0.5 | − 0.098*** | | | |
| | SAR model | RelElev | 0.026*** | 1035 | 0.319 | − 359.9 |
| | | Intercept | − 4.057*** | | | |
| | | Eca0.5 | − 0.043*** | | | |
| D | OLS linear model | RelElev | 0.011*** | 836 | 0.109 | 188.3 |
| | | Intercept | − 6.129*** | | | |
| | | Eca1 | − 0.029*** | | | |
| | | RelElev | 0.015*** | | | |
| | | Slope | − 0.026*** | | | |
| | SAR model | TWI | 0.022** | 833 | 0.300 | 104.0 |
| | | Intercept | − 3.482*** | | | |
| | | RelElev | 0.008*** | | | |
| | | Slope | − 0.011*** | | | |
| | | TWI | 0.015** | | | |
| A + B + C + D | OLS linear model | Intercept | 1.233*** | 3837 | 0.344 | 523.3 |
| | | Eca0.5 | − 0.083*** | | | |
| | | Eca1 | 0.020*** | | | |
| | | Elev | − 0.001*** | | | |
| | | RelElev | 0.006*** | | | |
| | | Slope | − 0.018*** | | | |
| | | TPI | − 0.102** | | | |
| | SAR model | Intercept | 0.305*** | 3837 | 0.582 | − 216.2 |
| | | Eca0.5 | − 0.019*** | | | |
| | | Elev | − 0.0003*** | | | |
| | | Slope | − 0.006*** | | | |
| | | | | | | |

Where Eca0.5 and Eca1 are the soil apparent electrical conductivity at 0.5 and 1 m of soil depth, respectively, TWI is the topographic wetness index, TPI is the topographic position index, TRI is the topographic roughness index. * $P < 0.05$; ** $P < 0.01$; *** $P < 0.001$

Table 6 Statistics of spatial dependence of OLS fitting residuals for model selection, using Lagrange multiplier and SARMA tests, for each local model (A, B, C and D) and the general model (A + B + C + D)

| Test | A | B | C | D | A + B + C + D |
|------------------------|-----------|------------|------------------------------|------------------------------|------------------------------|
| Residuals Moran's I | 3.898*** | 4.843*** | 6.968*** | 9.101*** | 26.849*** |
| SLM | 7.712** | 12.276** | 44.979*** | 90.569*** | 745.790*** |
| SEM | 17.500*** | 34.738*** | 43.391*** | 81.573*** | 718.600*** |
| Robust SLM | 0.157 | 3.537 | 1.789 | 14.038*** | 42.486*** |
| robust SEM | 9.937** | 25.999*** | 0.201 | 5.0417* | 15.303*** |
| SARMA | 17.657*** | 38.275*** | 45.18*** | 95.611*** | 761.09*** |
| Likelihood ratio tests | SAC = SEM | SAC > SEM* | SAC > SLM*** SAC > SEM*** | SAC > SLM*** SAC > SEM*** | SAC > SLM*** SAC > SEM*** |

Where * $P < 0.05$; ** $P < 0.01$; *** $P < 0.001$; SAC = SEM indicates both models perform equally well; SAC > SLM or SAC > SEM indicates SAC model performs better than SLM or SEM, according to Likelihood ratio tests

other approaches, probably due to considering a larger number and more distant neighbours (Online Resource 1). Stand D, much younger and with lower *du* values, had a lower number of neighbours due to smaller individual influence areas and showed closer results compared to the contiguity and distance-based metrics. (Table 4).

The extent of identified *idu* spatial patterns varied between short distances (stand A) to much wider radius patterns (stand C), showing the in-site variability of tree development that may be found on cork oak high-density plantations. The lower spatial autocorrelation was observed where the tested edaphic and topographic variables had a lower relation with *idu*, hinting that the spatial variation of these variables in stands C and D may be responsible for the presence of more evident spatial patterns.

All fitted spatial models improved their respective OLS versions. The considerable improvement of predictive capacity in fitted models proves that its advantageous integrating the spatial autocorrelation when modelling cork oak *idu*, particularly when stronger spatial autocorrelation is present. The spatial approach has potential for a more accurate modelling and prediction of individual tree diameter development, which shows that intra-stand variability is an important aspect to consider for management decisions.

The SEM outperformed the SLM on stands A and B, but on the contrary, SLM had slightly better scores in stands C and D. In fact, in stand A the source of autocorrelation related to the influence from neighbours (ρ parameter) was residual, making SEM a better choice. In this stand the existing spatial autocorrelation was associated with the error term, suggesting that other factors not considered in our OLS model may be responsible for this spatial autocorrelation. A similar assumption could be made for stand B, even though SAR was chosen. Stands C and D showed similar scores for both types of spatial autocorrelation. The stronger positive ρ parameter suggests that trees are responding similarly to the underlying spatial patterns, and these patterns are partially explained in the models, potentially reducing the λ parameter, which was verified on the higher predictive capacity on the OLS models.

Although our results show that modelling autocorrelation is very useful, the practical requirement of acquiring the precise position and measurement of every tree diameter in wide areas can be challenging. To avoid this problem, remote sensing techniques based on precision photography or LiDAR data could be used for acquiring tree position, as well

as obtaining tree size metrics as tree height or canopy size (Surový et al. 2018; Simonson et al. 2018).

Effect of edaphic and topographic variables on growth modelling

This study successfully used edaphic and topographic data, obtained from digital mapping methods, to explore its fine-scale relationships with individual trees of cork oak under high-density young plantations. We observed that despite each local spatial and non-spatial model showing differences in the final set of variables included as statistically significant, the parameter values presented a consistent effect in relation to the response variable *idu*. This observation was then supported by the parameter values of the general model, and therefore coped with the larger variability of the explanatory variables but also with the higher variability of tree *du* and *idu*.

When analyzing the selected general model, we noticed that at least a variable related to soil, topography and elevation were kept, evidencing these different characteristics are simultaneously relevant to tree growth. In fact, these fitted models, in particular the spatial model, showed a good predictive capacity based solely on these variables and the respective range of values we observed. It should be noted, however, that the fitted model should be considered with caution, as it is limited by the range of explanatory variables used and by the average to high site index. Further testing this methodology in more stands with more variability of site conditions could reinforce our finding and contribute to improved general model, based on wider edaphic and topographic conditions.

The differences in precipitation and soil characteristics may constitute a determining factor on the soil–water–topography dynamics. Stands A and B, located in the drier region, were constituted predominantly by sandy soils, known as very favourable to cork oak species (Costa et al. 2008; Paulo et al. 2015). These soils have higher permeability and thus lower water storage capacity, which can constrain cork oak growth due the lack of water in the Mediterranean dry season, but exhibit high soil depths and unconsolidated parent material, favourable to root development and access to groundwater (Fisher and Binkley 2000). In fact, according to our soil profile examination, the usable soil layer was thinner in stands C and D, likely constraining root development. These considerable soil differences may change the effect of water retention as deficient drainage can lead to flooding, known to be associated to a reduction of root respiration rates (Kozłowski 1984), and increased dissemination of pests such as *Phytophthora cinnamomi* (Moreira and Martins 2005).

CEa variables had an important role in describing cork oak development. CEa parameters were significant in three of the four studied stands and in the A+B+C+D model. In fact, the linear regression with CEa0.5 as predictor explained 11.34% of *idu* variability in stand C and 2.76% in stand D. We observed that CEa0.5 estimates were negative in any model, while the parameter estimates associated to CEa at 1 m were positive except on stand D, showing an opposite effect of cork oak growth at the two soil depths. CEa interpretation may be complex since it depends on several factors such as soil texture, salinity, cation exchange capacity or temperature (Corwin and Lesch 2005). According to previous studies, as long as soils are non-saline ECa is well related with soil texture (Corwin and Lesch 2005; Sudduth et al. 2017; Plant 2019), with higher ECa value being observed in finer textures. This suggests that coarser textures benefit cork oak growth at 0.5 m of soil depth while the opposite is observed at 1 m for the studied soils. Due to this complexity, soil samples may be taken additionally to identify the specific nutrients/organic matter relations with CEa in a specific stand soil (Johnson et al. 2005). In this study, the goal

was understanding the role and reliability of CEa on explaining spatial differences on cork oak development. To further advance on this subject, a study dedicated to understanding what factors are correlated to CEa variability in each stand, and then tree growth, would be needed.

The two elevation variables showed distinct impacts on *idu*. RelElev, representing the elevation fine-scale standardised variations was not significant in the sandy soil and smoother topographic stands, but a positive relation to *idu* was observed in stands C and D. Fricker et al. (2019) and Príncipe et al. (2022) showed the importance of elevation at finer scales to tree development, as proxy to microclimatic conditions as water availability, solar radiation or wind exposure. Our results are in accordance with the existence of microclimatic differences, but with the relation to tree development depending on soil depth and potential water drainage on less elevated zones. Elev, the elevation above sea level, showing a negative relation to *idu* instead. The interpretation of this result is complex, as the variable integrates the geographic location and macroclimatic variations between stands, which ultimately affect cork oak productivity. In that sense, it indicates stands C and D higher altitudes combined with geographic location have less conditions for cork oak development, which is corroborated by (Paulo et al. 2015).

Slope was found to have a negative relation with *idu*, meaning steeper slopes being less adequate to cork oak growth, which is in accordance to Costa et al. (2010), even if the used slope range was limited to smooth hillsides. The same negative relation was observed with TPI, showing that trees in higher positions relative to their neighbours had lesser *idu*.

TWI, a variable that expresses the potential soil moisture based on elevation and slope conditions, was only significant in stands A and D. For both, the parameter estimates showed a positive relationship with *idu* suggesting the more humid locations benefit observed tree growth, which agrees with (Costa et al. 2008). One could expect a negative relation between TWI and tree growth, due to the potential for periods of waterlogging of the studied stands. On one side, cork oak species has tolerance for wetter soils, and thus higher TWI (Petroselli et al. 2013), on the other side, the negative effects of water excess on tree development may be underlooked in these results, being expressed as mortality instead of growth.

Our study focuses on variables which could be digitally mapped with a low cost and logistic effort, testing if such a method could present a reliable and easy way to obtain information to aid afforestation and forest management plans. We did not explore the potential of intraspecific competition as a factor influencing either tree growth or the spatial autocorrelation process. This decision was made based on the findings of Faias et al. (2020) and Firmino et al. (2023), who investigated intraspecific competition using inventory plots, including those on these stands, and found no evidence of competition impacting tree growth. Over time, the competition effect is likely to increase and cause dissimilarity between neighbouring trees (Pommerening and Sánchez-Meador 2018), in contrast to the spatial effect from microsite conditions. Also, we did not access the spatial variation of soil under 1 m or mapped usable soil depth for the whole areas, which we observed to vary considerably at least in stand C according to soil profiles. Such variables are of interest as the primary cork oak root system is developed to reach lower soil levels, accessing groundwater and minerals that are likely unreachable by neighbour trees (Moreno et al. 2005; David et al. 2007). Mortality was also not explored and likely could complement this analysis. Factors underlying tree cork oak mortality represent an important problem (e.g. Torres 2008; Costa et al. 2010; Alves 2014) and a study of spatial analysis of these factors could bring vital information to its knowledge.

Conclusion

Edaphic and topographic microsite conditions exhibited a weak correlation to cork oak diameter growth, when the analysis was carried out on each stand separately, in particular in the stands characterised by sandy soils and smooth topographic variations. The correlation increased to moderate in the stands where topographic variations were higher, which combined with lower soil depth, potentially became restrictive for cork oak development. When stands were observed together, the increase of the range of site conditions allowed a better observation on the relationship of the variables with diameter growth, namely ECa0.5, Elev and Slope. These variations should, therefore, be accessed when defining management plans for new plantations, as they may influence the success and productivity of the stands.

The presence of spatial diameter growth patterns varied between stands, being possibly accentuated by more restrictive site conditions, related to the resource variation at a micro-scale. Integrating this spatial autocorrelation overall improved diameter growth modelling when compared to ordinary linear models, even though they reveal essentially the same set of predictors. The fitted general spatial model showed a substantial predictive capacity of $R^2=0.58$, which suggests that spatial statistical approaches are of interest to improve modelling and an improved understanding of relationships between drivers and growth in cork oak plantations. However, the fitted models are based on medium to high site index stands and should be considered with caution outside this range.

Supplementary Information The online version contains supplementary material available at <https://doi.org/10.1007/s11056-024-10047-9>.

Acknowledgements Centro de Estudos Florestais is a research unit funded by Fundação para a Ciência e Tecnologia (FCT) (UIDB/00239/2020). First author was financed by FCT under the contract SFRH/BD/133598/2017. Second author was financed by FCT under the contract SFRH/BPD/96475/2013. We thank the respective private forest owners for cooperating and allowing data collecting on their properties. We thank Area400 for the cooperation in soil digital data collection. We thank Catarina Jorge, Inês Bento, Jean Magalhães, Phuong Nguyen and Valentine Aubard for the help in biometric tree data collection.

Author contributions Conceptualization: J.A.P., M.C., P.N.F.; Methodology: A.L., J.A.P., M.C., P.N.F.; Formal analysis: J.A.P., M.C., M.T., P.N.F.; Writing—Original Draft Preparation: P.N.F.; Writing—Review & Editing: A.L., J.A.P., M.C., M.T., P.N.F.; Funding Acquisition: J.A.P., M.T., P.N.F. All authors have read and agreed to the published version of the manuscript.

Funding Open access funding provided by FCTIFCCN (b-on).

Data availability No datasets were generated or analysed during the current study.

Declarations

Competing interests The corresponding author, on behalf of the authors of this manuscript, declare that there are no competing interests.

Open Access This article is licensed under a Creative Commons Attribution 4.0 International License, which permits use, sharing, adaptation, distribution and reproduction in any medium or format, as long as you give appropriate credit to the original author(s) and the source, provide a link to the Creative Commons licence, and indicate if changes were made. The images or other third party material in this article are included in the article's Creative Commons licence, unless indicated otherwise in a credit line to the material. If material is not included in the article's Creative Commons licence and your intended use is not permitted by statutory regulation or exceeds the permitted use, you will need to obtain permission directly from the copyright holder. To view a copy of this licence, visit <http://creativecommons.org/licenses/by/4.0/>.

References

- AIFF (2010) Relatório de caracterização da fileira florestal. Associação Para a Competitividade da Indústria da Fileira Florestal: Lisboa, Portugal
- Alves C (2014) Studies on cork oak decline: A integrated approach. Ph.D. Thesis, Évora University
- Andivia E, Fernández M, Alejano R, Vázquez-Piqué J (2015) Tree patch distribution drives spatial heterogeneity of soil traits in cork oak woodlands. *Ann for Sci* 72:549–559. <https://doi.org/10.1007/s13595-015-0475-8>
- Anselin L, Bera AK (1998) spatial dependence in linear regression models with an introduction to spatial econometrics. In: Ullah A (ed) *Handbook of applied economic statistics*. Marcel Dekker, New York, pp 237–289
- Anselin L, Bera AK, Florax R, Yoon MJ (1996) Simple diagnostic tests for spatial dependence. *Reg Sci Urban Econ* 26:77–104. [https://doi.org/10.1016/0166-0462\(95\)02111-6](https://doi.org/10.1016/0166-0462(95)02111-6)
- Besson CK, Lobo-do-Vale R, Rodrigues ML, Almeida P, Herd A, Grant OM, David TS, Schmidt M, Otieno D, Keenan TF, Gouveia C, Mériaux C, Chaves MM, Pereira JS (2014) Cork oak physiological responses to manipulated water availability in a Mediterranean woodland. *Agric for Meteorol* 184:230–242. <https://doi.org/10.1016/j.agrformet.2013.10.004>
- Beven KJ, Kirkby MJ (1979) A physically based, variable contributing area model of basin hydrology. *Hydrol Sci Bull* 24:43–69. <https://doi.org/10.1080/02626667909491834>
- Bivand R, Millo G, Piras G (2021) A review of software for spatial econometrics in r. *Mathematics* 9:1–40. <https://doi.org/10.3390/math9111276>
- Bivand RS, Pebesma E, Gómez-Rubio V (2013) *Applied spatial data analysis with R*, 2nd edn. Springer, New York
- Bivand RS, Wong DWS (2018) Comparing implementations of global and local indicators of spatial association. *TEST* 27:716–748. <https://doi.org/10.1007/s11749-018-0599-x>
- Brown R, Fredericksen T (2008) Topographic factors affecting the tree species composition of forests in the upper piedmont of Virginia. *Va J Sci*. <https://doi.org/10.25778/1sm7-xg66>
- Bullock BP, Burkhardt HE (2005) An evaluation of spatial dependency in juvenile loblolly pine stands using stem diameter. *For Sci* 51:102–108. <https://doi.org/10.1093/forestscience/51.2.102>
- Cerasoli S, Campagnolo M, Faria J, Nogueira C, Da Conceição CM (2018) On estimating the gross primary productivity of Mediterranean grasslands under different fertilization regimes using vegetation indices and hyperspectral reflectance. *Biogeosciences* 15:5455–5471. <https://doi.org/10.5194/bg-15-5455-2018>
- Coelho MB, Paulo JA, Palma JHN, Tomé M (2012) Contribution of cork oak plantations installed after 1990 in Portugal to the Kyoto commitments and to the landowners economy. *For Policy Econ* 17:59–68. <https://doi.org/10.1016/j.forpol.2011.10.005>
- Corwin DL, Lesch SM (2005) Apparent soil electrical conductivity measurements in agriculture. *Comput Electron Agric* 46:11–43. <https://doi.org/10.1016/j.compag.2004.10.005>
- Costa A, Madeira M, Oliveira ÂC (2008) The relationship between cork oak growth patterns and soil, slope and drainage in a cork oak woodland in Southern Portugal. *For Ecol Manage* 255:1525–1535. <https://doi.org/10.1016/j.foreco.2007.11.008>
- Costa A, Oliveira AC (2001) Variation in cork production of the cork oak between two consecutive cork harvests. *Forestry* 74:337–346. <https://doi.org/10.1093/forestry/74.4.337>
- Costa A, Pereira H, Madeira M (2009) Landscape dynamics in endangered cork oak woodlands in South-western Portugal (1958–2005). *Agrofor Syst* 77:83–96. <https://doi.org/10.1007/s10457-009-9212-3>
- Costa A, Pereira H, Madeira M (2010) Analysis of spatial patterns of oak decline in cork oak woodlands in Mediterranean conditions. *Ann for Sci* 67:204–204. <https://doi.org/10.1051/forest/2009097>
- David TS, Henriques MO, Kurz-Besson C, Nunes J, Valente F, Vaz M, Pereira JS, Siegwolf R, Chaves MM, Gazarini LC, David JS (2007) Water-use strategies in two co-occurring Mediterranean evergreen oaks: surviving the summer drought. *Tree Physiol* 27:793–803. <https://doi.org/10.1093/treephys/27.6.793>
- Davis FW, Goetz S (1990) Modeling vegetation pattern using digital terrain data. *Landsc Ecol* 4:69–80. <https://doi.org/10.1007/BF02573952>
- Dettori S, Filigheddu MR, Deplano G, Molgora JE, Ruiu M, Sedda L (2018) Employing a spatio-temporal contingency table for the analysis of cork oak cover change in the Sa Serra region of Sardinia. *Sci Rep* 8:1–14. <https://doi.org/10.1038/s41598-018-35319-1>
- Dinis C (2014) Cork oak (*Quercus suber* L.) root system: a structural-functional 3D approach. Ph.D. Thesis, Évora University.
- Doerge T, Kitchen NR, Lund ED (1999) Soil electrical conductivity mapping. *Crop Insights* 9:1–4
- Domsch H, Giebel A (2004) Estimation of soil textural features from soil electrical conductivity recorded using the EM38. *Precis Agric* 5:389–409. <https://doi.org/10.1023/B:PRAG.0000040807.18932.80>

- Faias SP, Paulo JA, Firmino PN, Tomé M (2019) Drivers for annual cork growth under two understory management alternatives on a podzolic cork oak stand. *Forests* 10:1–13. <https://doi.org/10.3390/f10020133>
- Faias SP, Paulo JA, Tomé M (2020) Inter-tree competition analysis in undebarked cork oak plantations as a support tool for management in Portugal. *New for* 51:489–505. <https://doi.org/10.1007/s11056-019-09739-4>
- Firmino PN, Tomé M, Paulo JA (2023) Do distance-dependent competition indices contribute to improve diameter and total height tree growth prediction in juvenile cork oak plantations? *Forests*. <https://doi.org/10.3390/f14051066>
- Fisher FR, Binkley D (2000) *Ecology and management of forest soils*, 3rd edn. Wiley, New York
- Fortin MJ, Dale MRT (2005) *Spatial analysis: a guide for ecologists*, 2nd edn. Cambridge University Press, New York
- Fox J, Weisberg S (2019) *An R companion to applied regression*, 3rd edn. Sage, Thousand Oaks
- Fricker GA, Synes NW, Serra-Diaz JM, North MP, Davis FW, Franklin J (2019) More than climate? Predictors of tree canopy height vary with scale in complex terrain, Sierra Nevada, CA (USA). *For Ecol Manag* 434:142–153. <https://doi.org/10.1016/j.foreco.2018.12.006>
- Furnival GM, Wilson RW (1974) Regressions by leaps and bounds. *Technometrics* 16:499–511. <https://doi.org/10.2307/1267601>
- Gea-Izquierdo G, Cañellas I (2009) Analysis of holm oak intraspecific competition using gamma regression. *For Sci* 55:310–322. <https://doi.org/10.1093/forestscience/55.4.310>
- Getzin S, Wiegand T, Wiegand K, He F (2008) Heterogeneity influences spatial patterns and demographics in forest stands. *J Ecol* 96:807–820. <https://doi.org/10.1111/j.1365-2745.2008.01377.x>
- Heil K, Schmidhalter U (2017) The application of EM38: determination of soil parameters, selection of soil sampling points and use in agriculture and archaeology. *Sensors*. <https://doi.org/10.3390/s17112540>
- ICNF (2019) Relatório Final do 6.º Inventário Florestal Nacional. Instituto da Conservação da Natureza e Florestas.
- IUSS Working Group WRB (2006) *World reference base for soil resources*, 2nd edn. World Soil Resources Reports, Rome
- Johnson CK, Eskridge KM, Corwin DL (2005) Apparent soil electrical conductivity: applications for designing and evaluating field-scale experiments. *Comput Electron Agric* 46:181–202. <https://doi.org/10.1016/j.compag.2004.12.001>
- Kozłowski TT (1984) Plant responses to flooding of soil. *Bioscience* 34:162–167. <https://doi.org/10.2307/1309751>
- Kühn J, Brenning A, Wehrhan M, Koszinski S, Sommer M (2009) Interpretation of electrical conductivity patterns by soil properties and geological maps for precision agriculture. *Precis Agric* 10:490–507. <https://doi.org/10.1007/s11119-008-9103-z>
- Lecomte X, Paulo JA, Tomé M, Veloso S, Firmino PN, Faias SP, Caldeira MC (2022) Shrub understorey clearing and drought affects water status and growth of juvenile *Quercus suber* trees. *For Ecol Manag* 503:119760. <https://doi.org/10.1016/j.foreco.2021.119760>
- Legendre P, Fortin MJ (1989) Spatial pattern and ecological analysis. *Vegetatio* 80:107–138. <https://doi.org/10.1007/BF00048036>
- Li Y, Yang H, Wang H, Ye S, Liu W (2019) Assessing the influence of the minimum measured diameter on forest spatial patterns and nearest neighborhood relationships. *J Mt Sci* 16:2308–2319. <https://doi.org/10.1007/s11629-019-5540-6>
- Lindsay JB (2016) Whitebox GAT: a case study in geomorphometric analysis. *Comput Geosci* 95:75–84. <https://doi.org/10.1016/j.cageo.2016.07.003>
- Lumley T (2009) *Leaps: regression subset selection*, R package version 2.9. <https://cran.r-project.org/web/packages/leaps/leaps.pdf>
- Machado FC, Montanari R, Shiratsuchi LS, Lovera LH, de Lima ES (2015) Spatial dependence of electrical conductivity and chemical properties of the soil by electromagnetic induction. *Rev Bras Cienc Do Solo* 39:1112–1120. <https://doi.org/10.1590/01000683rbcs20140794>
- Maleki K, Zeller L, Pretzsch H (2020) Oak often needs to be promoted in mixed beech-oak stands—the structural processes behind competition and silvicultural management in mixed stands of European beech and sessile oak. *Iforest* 13:80–88. <https://doi.org/10.3832/ifor3172-013>
- Mcbride S, Nguyen ML, Rickard DS (1990) Implications of ceasing annual superphosphate topdressing applications on pasture production. *Proc New Zeal Grassl Assoc* 180:177–180. <https://doi.org/10.33584/jnzg.1990.52.1978>
- Moran PAP (1950) Notes on continuous stochastic phenomena. *Biometrika* 37:17–23. <https://doi.org/10.2307/2332142>
- Moreira AC, Martins JMS (2005) Influence of site factors on the impact of *Phytophthora cinnamomi* in cork oak stands in Portugal. *For Pathol* 35:145–162. <https://doi.org/10.1111/j.1439-0329.2005.00397.x>

- Moreno G, Obrador JJ, Cubera E, Dupraz C (2005) Fine root distribution in Dehesas of Central-Western Spain. *Plant Soil* 277:153–162. <https://doi.org/10.1007/s11104-005-6805-0>
- Myers RH (1990) Classical and modern regression with applications, 2nd edn. Duxbury Press, London
- Natividade JV (1950) Subericultura. Direção Geral dos Serviços Florestais e Aquícolas, Lisbon
- Neely HL, Morgan CLS, Hallmark CT, McInnes KJ, Molling CC (2016) Apparent electrical conductivity response to spatially variable vertisol properties. *Geoderma* 263:168–175. <https://doi.org/10.1016/j.geoderma.2015.08.040>
- Pace RK, LeSage JP (2003) Likelihood dominance spatial inference. *Geogr Anal* 35:133–147. <https://doi.org/10.1111/j.1538-4632.2003.tb01105.x>
- Paillet Y, Cassagne N, Brun JJ (2010) Monitoring forest soil properties with electrical resistivity. *Biol Fertil Soils* 46:451–460. <https://doi.org/10.1007/s00374-010-0453-0>
- Paulo JA, Firmino PN, Faias SP, Tomé M (2021) Quantile regression for modelling the impact of climate in cork growth quantiles in Portugal. *Eur J for Res* 140:991–1004. <https://doi.org/10.1007/s10342-021-01379-8>
- Paulo JA, Faias SP, Ventura-Giroux C, Tomé M (2016) Estimation of stand crown cover using a generalized crown diameter model: application for the analysis of portuguese cork oak stands stocking evolution. *Iforest* 9:437–444. <https://doi.org/10.3832/ifor1624-008>
- Paulo JA, Palma JHN, Gomes AA, Faias SP, Tomé J, Tomé M (2015) Predicting site index from climate and soil variables for cork oak (*Quercus suber* L.) stands in Portugal. *New for* 46:293–307. <https://doi.org/10.1007/s11056-014-9462-4>
- Paulo JA, Tomé M (2009) An individual tree growth model for juvenile cork oak stands in southern Portugal. *Silva Lusit* 17:27–38
- Paulo JA, Tomé M (2014) Estimativa das Produções de Cortiça Virgem Resultantes das Operações de Desbastes e Desboia em Montados de Sobreiro em Fase Juvenil. *Silva Lusit* 22:29–42
- Paulo MJ, Stein A, Tomé M (2002) A spatial statistical analysis of cork oak competition in two Portuguese silvopastoral systems. *Can J for Res* 32:1893–1903. <https://doi.org/10.1139/x02-107>
- Pommerening A, Sánchez-Meador AJ (2018) Tamm review: tree interactions between myth and reality. *For Ecol Manag* 424:164–176. <https://doi.org/10.1016/j.foreco.2018.04.051>
- Surový P, Ribeiro NA, Panagiotidis D (2018) Estimation of positions and heights from UAV-sensed imagery in tree plantations in agrosilvopastoral systems. *Int J Remote Sens* 39:4786–4800. <https://doi.org/10.1080/01431161.2018.1434329>
- Petrutan AM, Biris IA, Merce O, Turcu DO, Petritan IC (2012) Structure and diversity of a natural temperate sessile oak (*Quercus petraea* L.) - European Beech (*Fagus sylvatica* L.) forest. *For Ecol Manag* 280:140–149. <https://doi.org/10.1016/j.foreco.2012.06.007>
- Petroselli A, Vessella F, Cavagnuolo L, Piovesan G, Schirone B (2013) Ecological behavior of *Quercus suber* and *Quercus ilex* inferred by topographic wetness index (TWI). *Trees Struct Funct* 27:1201–1215. <https://doi.org/10.1007/s00468-013-0869-x>
- Plant RE (2019) Spatial data analysis in ecology and agriculture using R, 2nd edn. CRC Press, New York
- Príncipe A, Nunes A, Pinho P, Aleixo C, Neves N, Branquinho C (2022) Local-scale factors matter for tree cover modelling in Mediterranean drylands. *Sci Total Environ* 831:154877. <https://doi.org/10.1016/j.scitotenv.2022.154877>
- R Core Team (2021) R: A language and environment for statistical computing. R Foundation for Statistical Computing, Vienna, Austria. <https://www.R-project.org/>
- Reed DD, Burkhart HE (1985) Spatial autocorrelation of individual tree characteristics in loblolly pine stands. *For Sci* 31:575–587
- Riley SJ, DeGloria SD, Elliot R (1999) A terrain ruggedness index that quantifies topographic heterogeneity. *Interm J Sci* 5:23–27
- Rocha J, Duarte A, Silva M, Fabres S, Vasques J, Revilla-Romero B, Quintela A (2020) The importance of high resolution digital elevation models for improved hydrological simulations of a mediterranean forested catchment. *Remote Sens* 12:1–17. <https://doi.org/10.3390/rs12203287>
- Rodrigues AC, Villa PM, Ferreira-Júnior WG, Schaefer CERG, Neri AV (2021) Effects of topographic variability and forest attributes on fine-scale soil fertility in late-secondary succession of Atlantic Forest. *Ecol Process* 10:1–9. <https://doi.org/10.1186/s13717-021-00333-1>
- Rudolph S, Wonglecharoen C, Lark RM, Marchant BP, Garré S, Herbst M, Vereecken H, Weihermüller L (2016) Soil apparent conductivity measurements for planning and analysis of agricultural experiments: a case study from Western-Thailand. *Geoderma* 267:220–229. <https://doi.org/10.1016/j.geoderma.2015.12.013>

- Salinas-Melgoza MA, Skutsch M, Lovett JC (2018) Predicting aboveground forest biomass with topographic variables in human-impacted tropical dry forest landscapes. *Ecosphere*. <https://doi.org/10.1002/ecs2.2063>
- Sampaio T, Gonçalves E, Faria C, Almeida MH (2021) Genetic variation among and within *Quercus suber* L. populations in survival, growth, vigor and plant architecture traits. *For Ecol Manag* 483:118715. <https://doi.org/10.1016/j.foreco.2020.118715>
- Sánchez-González M, Tomé M, Montero G (2005) Modelling height and diameter growth of dominant cork oak trees in Spain. *Ann for Sci* 62:633–643. <https://doi.org/10.1051/forest>
- Sedda L, Atkinson PM, Filigheddu MR, Cotzia G, Dettori S (2011) Spatio-temporal analysis of tree height in a young cork oak plantation. *Int J Geogr Inf Sci* 25:1083–1096. <https://doi.org/10.1080/13658816.2010.517534>
- Sedda L, Dettori S (2006) Analisi variografica del diametro di un impianto di quercia da sughero. Un esempio di studio della corregionalizzazione in ambito forestale. *L'italia for e Mont*. <https://doi.org/10.4129/ifm.2006.6.04>
- Simonson W, Allen H, Coomes D (2018) Effect of tree phenology on lidar measurement of Mediterranean forest structure. *Remote Sens* 10:1–13. <https://doi.org/10.3390/rs10050659>
- Sudduth KA, Kitchen NR, Drummond ST (2017) Inversion of soil electrical conductivity data to estimate layered soil properties. *Adv Anim Biosci* 8:433–438. <https://doi.org/10.1017/s2040470017001303>
- Tome M, Burkhart HE (1989) Distance-dependent competition measures for predicting growth of individual trees. *For Sci* 35:816–831. <https://doi.org/10.1093/forestscience/35.3.816>
- Torres E (2008) Cork oak woodlands on the edge: ecology, adaptive management, and restoration. *Restor Ecol* 18:615–617. <https://doi.org/10.1111/j.1526-100x.2010.00701.x>
- Vessella F, López-Tirado J, Simeone MC, Schirone B, Hidalgo PJ (2017) A tree species range in the face of climate change: cork oak as a study case for the Mediterranean biome. *Eur J Res* 136:555–569. <https://doi.org/10.1007/s10342-017-1055-2>
- Walker LR, del Moral R (2003) Primary succession and ecosystem rehabilitation. Cambridge University Press, London
- Wilson MFJ, O'Connell B, Brown C, Guinan JC, Grehan AJ (2007) Multiscale terrain analysis of multi-beam bathymetry data for habitat mapping on the continental slope. *Mar Geodesy* 30:3–35. <https://doi.org/10.1080/01490410701295962>

Publisher's Note Springer Nature remains neutral with regard to jurisdictional claims in published maps and institutional affiliations.

Authors and Affiliations

Paulo Neves Firmino¹  · Joana Amaral Paulo²  · António Lourenço³ · Margarida Tomé²  · Manuel Campagnolo² 

✉ Paulo Neves Firmino
pnfirmino@isa.ulisboa.pt

Joana Amaral Paulo
joanaap@isa.ulisboa.pt

António Lourenço
antoniolourenco@agro-analitica.com

Margarida Tomé
magatome@isa.ulisboa.pt

Manuel Campagnolo
mlc@isa.ulisboa.pt

¹ Forest Research Centre, School of Agriculture, University of Lisbon, Tapada da Ajuda, 1349-017 Lisbon, Portugal

² Forest Research Centre, Associated Laboratory TERRA, School of Agriculture, University of Lisbon, Tapada da Ajuda, 1349-017 Lisbon, Portugal

³ Agro Analítica, Consulting Company, Avenida Infante Santo, 23 4A, 1350-115 Lisbon, Portugal